Experimental comparison of coherent polarization-switched QPSK to polarization-multiplexed QPSK for 10 × 100 km WDM transmission

L. E. Nelson,[1,*] X. Zhou,[1] N. Mac Suibhne,[2] A. D. Ellis,[2] and P. Magill[1]

[1]*AT&T Labs – Research, 200 South Laurel Avenue, Middletown, New Jersey 07748, USA*
[2]*Tyndall National Institute, University College Cork, Cork, Ireland*
**lenelson@research.att.com*

Abstract: Polarization-switched quadrature phase-shift keying has been demonstrated experimentally at 40.5Gb/s with a coherent receiver and digital signal processing. Compared to polarization-multiplexed QPSK at the same bit rate, its back-to-back sensitivity at 10^{-3} bit-error-ratio shows 0.9dB improvement, and it tolerates about 1.6dB higher launch power for 10 × 100km, 50GHz-spaced WDM transmission allowing 1dB penalty in required optical-signal-to-noise ratio relative to back-to-back.

OCIS codes: (060.2330) Fiber optics communications; (060.1660) Coherent communications. (060.4080) Modulation.

References and links

1. D. Qian, M.-F. Huang, E. Ip, Y.-K. Huang, Y. Shao, J. Hu, and T. Wang, "101.7-Tb/s (370x294-Gb/s) PDM-128QAM –OFDM transmission over 3x55-km SSMF using pilot-based phase noise mitigation," Proc. OFC-NFOEC 2011, Los Angeles, CA, paper PDPB5.
2. X. Zhou, L. E. Nelson, P. Magill, R. Isaac, B. Zhu, D. W. Peckham, P. Borel, and K. Carlson, "8x450Gb/s, 50-GHz-spaced, PDM-32QAM transmission over 400km and one 50GHz ROADM," Proc. OFC-NFOEC 2011, Los Angeles, CA, paper PDPB3.
3. M. Karlsson, and E. Agrell, "Which is the most power-efficient modulation format in optical links?" Opt. Express **17**(13), 10814–10819 (2009).
4. E. Agrell, and M. Karlsson, "Power efficient modulation formats in coherent transmission systems," J. Lightwave Technol. **27**(22), 5115–5126 (2009).
5. H. Bülow, "Polarization QAM modulation (POLQAM) for coherent detection schemes," Proc. OFC-NFOEC 2009, San Diego, CA, paper OWG2.
6. P. Poggiolini, G. Bosco, A. Carena, V. Curri, and F. Forghieri, "Performance evaluation of coherent WDM PS-QPSK (HEXA) accounting for non-linear fiber propagation effects," Opt. Express **18**(11), 11360–11371 (2010).
7. P. Serena, A. Vannucci, and A. Bononi, "The performance of polarization switched QPSK (PS-QPSK) in dispersion managed WDM transmissions," in Proc. of ECOC'2010, paper Th.10.E.2.
8. E. Masalkina, R. Dischler, and H. Bülow, "Experimental study of polarization-switched-QPSK subcarrier modulation and iterative demapping on optical OFDM systems," in Proc. of OFC-NFOEC 2011, paper OThO6.
9. M. Sjödin, P. Johannisson, H. Wymeersch, P. A. Andrekson, and M. Karlsson, "Comparison of polarization-switched QPSK and polarization-multiplexed QPSK at 30 Gbit/s," Opt. Express **19**(8), 7839–7846 (2011).
10. P. Johannisson, M. Sjödin, M. Karlsson, H. Wymeersch, E. Agrell, and P. A. Andrekson, "Modified constant modulus algorithm for polarization-switched QPSK," Opt. Express **19**(8), 7734–7741 (2011).
11. D. S. Millar, D. Lavery, S. Makovejs, C. Behrens, B. C. Thomsen, P. Bayvel, and S. J. Savory, "Generation and long-haul transmission of polarization-switched QPSK at 42.9 Gb/s," Opt. Express **19**(10), 9296–9302 (2011).
12. D. S. Millar, and S. J. Savory, "Blind adaptive equalization of polarization-switched QPSK modulation," Opt. Express **19**(9), 8533–8538 (2011).
13. D. N. Godard, "Self-recovering equalization and carrier tracking in two-dimensional data communication systems," IEEE Trans. Commun. **28**(11), 1867–1875 (1980).
14. X. Zhou, J. Yu, and P. D. Magill, "Cascaded two-modulus algorithm for blind polarization de-multiplexing of 114-Gb/s PDM-8-QAM optical signals," Proc. OFC-NFOEC 2009, San Diego, CA, paper OWG3.
15. X. Zhou, J. Yu, M. F. Huang, Y. Shao, T. Wang, L. Nelson, P. Magill, M. Birk, P. I. Borel, D. W. Peckham, R. Lingle, Jr., and B. Zhu, "64-Tb/s, 8 b/s/Hz, PDM-36QAM transmission over 320 km using both pre- and post-transmission digital signal processing," J. Lightwave Technol. **29**(4), 571–577 (2011).

#146424 - $15.00 USD Received 22 Apr 2011; revised 12 May 2011; accepted 12 May 2011; published 18 May 2011

16. X. Zhou, "An improved feed-forward carrier recovery algorithm for coherent receiver with M-QAM modulation format," IEEE Photon. Technol. Lett. **22**(14), 1051–1053 (2010).

1. Introduction

The push for higher spectral efficiencies to continue to lower the cost per transmitted bit for optical transport has focused significant recent research work on multi-level, multi-dimensional modulation formats to achieve the ultimate capacity in a single fiber. Continual progress has been made, with spectral efficiencies as high as 11 bit/s/Hz demonstrated using 128QAM at 294Gb/s [1] and 8.4bit/s/Hz using 32QAM at 400Gb/s [2]. However, due to the increased optical-signal-to-noise ratio (OSNR) requirements, the reach of these multi-level, multi-dimensional modulation formats is clearly a concern. Thus, power efficient modulation formats, those having a low required signal-to-noise ratio per bit for a given bit-error-ratio, have also garnered attention recently [3–5], with significant focus on four-dimensional optimized formats (i.e. those using both quadratures and both polarization components of the electromagnetic fields). Power-efficient modulation formats are of fundamental importance in optical communications because they provide the ultimate sensitivity limit for the optical channel. They also have practical importance because they enable increased nonlinear tolerance, and therefore the potential for ultra long-haul transmission. Karlsson and Agrell [3] first identified polarization-switched quadrature phase shift-keying (PS-QPSK) as the most power efficient format (disregarding formats with impractically low spectral efficiency for high-speed WDM systems). A 1.76dB better asymptotic sensitivity than binary PSK was predicted. However, in coded systems the sensitivity gains are, in general, lower, if the optimal FEC decoding technique that is specially designed for non-gray-coded system is not employed [5]. Other groups first simulated PS-QPSK's performance [6,7] for 100Gb/s WDM transmission and showed higher nonlinear tolerance compared to polarization-multiplexed (PM)-QPSK. Masalkina et al. [8] demonstrated PS-QPSK subcarrier modulation with iterative mapping on optical orthogonal-frequency-division-multiplexing. Recently, the Chalmers group reported the first experimental demonstration of PS-QPSK at 30Gb/s along with single-channel, 300km transmission [9] and reported a modified constant modulus algorithm for PS-QPSK [10]. In addition, Millar et al. [11] achieved long-haul WDM transmission of PS-QPSK at 42.9Gb/s in a re-circulating loop and showed a 30% reach increase over PM-QPSK.

In this paper, we report an experimental demonstration of the PS-QPSK format with coherent reception and digital signal processing (DSP) in a typical straight-line, 20-channel terrestrial WDM system and a comparison to polarization-multiplexed QPSK at the same bit rate of 40.5Gb/s. The low symbol rates of 13.5Gbaud for PS-QPSK and 10.125Gbaud for PM-QPSK were chosen so that bandwidth limitations of the transmitter/receiver components did not significantly impact the comparison. The PS-QPSK transmitter was implemented simply with a QPSK modulator followed by a polarization modulator. The performances of the modulation formats are compared in a single-channel back-to-back configuration, and for 10 × 100km WDM transmission over standard single-mode fiber with 50-GHz-spaced neighboring channels of the same modulation format, in both cases assuming hard-decision forward-error-correction. For PS-QPSK, in a parallel effort to that of [12], we developed a novel constrained multi-modulus algorithm, which has improved convergence performance to that reported in [10], because our algorithm inherently eliminates the convergence singularity problem. Results indicate a clear performance advantage of PS-QPSK over PM-QPSK, including 0.9dB sensitivity improvement for back-to-back (at 10^{-3} bit-error-ratio) and up to 1.6dB higher launch power tolerance.

2. Back-to-back sensitivity comparison

A simple setup was used for the investigation of the back-to-back sensitivities, as shown in Fig. 1. An external cavity laser (ECL) with ~100kHz linewidth at 1550nm is followed by a double-nested Mach-Zehnder modulator with a 3dB bandwidth >28GHz, to which 2^{15}-1

#146424 - $15.00 USD Received 22 Apr 2011; revised 12 May 2011; accepted 12 May 2011; published 18 May 2011

PRBS sequences are applied, amplified by drivers with 30GHz bandwidth. For PS-QPSK, the QPSK signal passes through a single-drive polarization modulator (Versawave PL-40G-5) having 40GHz bandwidth, where a 2π drive signal switches the polarization between two orthogonal states. For PM-QPSK the signal instead passes through a polarization-multiplexing stage consisting of a 3dB coupler, 30ns delay in one arm relative to the other, and polarization beam combiner. Amplified spontaneous emission from an erbium-doped fiber amplifier (EDFA) is added to the signal before it passes through two stages of amplification and filtering via wavelength blockers (WB) with 36GHz bandwidth. A standard polarization- and phase-diverse coherent receiver follows, consisting of a polarization-diverse 90° hybrid, a local oscillator (LO) of ~100kHz linewidth, and four balanced photo-detectors. A four-channel real-time sampling oscilloscope with 50GSa/s sample rate and 18GHz analog bandwidth performs the sampling and digitization (ADC), and a desktop computer then post-processes the captured data.

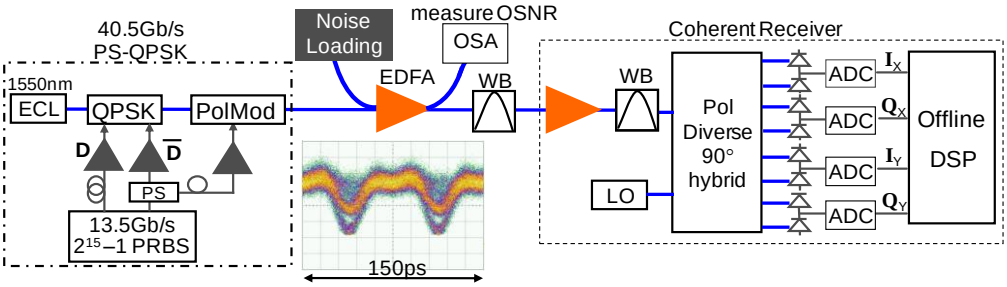

Fig. 1. Experimental set-up for PS-QPSK back-to-back measurements. The inset shows the PS-QPSK eye diagram. For PM-QPSK, a polarization multiplexing stage replaces the polarization modulator, and 10.125Gb/s data signals are applied to the QPSK modulator.

2.1 Receiver DSP algorithms

The flow chart diagram for the offline receiver DSP used in the experiment is shown in Fig. 2. After digital compensation of optical front-end errors (sampling skews and hybrid phase errors) and anti-aliasing filtering, the 50GSa/s signal is first down-sampled to (approximately) twice the baud rate. After that, the bulk chromatic dispersion (CD) is compensated using a frequency-domain static equalizer. Note that CD compensation was only used for the transmission experiments. The clock used to resample the signal is extracted by using the classic "square and filter method." Next, we perform simultaneous polarization recovery and residual CD compensation by using a 13-tap, T/2-spaced 2 × 2 adaptive equalizer. This adaptive equalizer is initialized by using decision-independent blind equalization algorithms (for pre-convergence), where the classic constant modulus algorithm (CMA) is used for PM-QPSK and a new constrained multi-modulus algorithm (MMA) is used for PS-QPSK. Once convergence is reached, the decision-independent algorithms switch to a decision-directed least-mean-square (DD-LMS) algorithm for steady-state operation. Note that, as also pointed out in [10,12], the traditional CMA [13] or multiple modulus algorithm (MMA) such as the cascaded MMA [14] cannot be used for polarization de-multiplexing of a PS-QPSK signal, because the signal components in the two orthogonal polarization states are correlated and the equalizer may converge to any combination of two phase-shifted QPSK signals. Similar to Millar et al. [12], our proposed constrained MMA exploits the signal correlation between the two orthogonal polarizations and de-multiplexes the PS-QPSK signal in each of the two orthogonal polarizations as a five-point constellation (1, j, −1, -j, 0), as can be seen in Fig. 3(b). Let Z_x (n) and Z_y(n) represent the equalized signals and R_x(n) and R_y(n) denote the expected square values of the radius/modulus of the constellation in the X- and Y-polarizations, respectively. The constrained MMA calculates the feedback errors from

#146424 - $15.00 USD Received 22 Apr 2011; revised 12 May 2011; accepted 12 May 2011; published 18 May 2011

$$\varepsilon_x(n) = |Z_x(n)|^2 - R_x(n), \qquad (1)$$
$$\varepsilon_y(n) = |Z_y(n)|^2 - R_y(n),$$

where

$$R_x(n) = E\left\{ |Z_x(n)|^2 + |Z_y(n)|^2 \right\} \text{ and } R_y(n) = 0, \text{ if } |Z_x(n)|^2 > |Z_y(n)|^2, \qquad (2)$$
$$R_x(n) = 0 \text{ and } R_y(n) = E\left\{ |Z_x(n)|^2 + |Z_y(n)|^2 \right\}, \text{ if } |Z_x(n)|^2 < |Z_y(n)|^2.$$

For the case when $|Z_x(n)| = |Z_y(n)|$, we let $\varepsilon_x = \varepsilon_y = 0$. Our experimental results have shown that the constrained MMA has very robust convergence performance and therefore can be used as either an independent blind equalization algorithm for PS-QPSK or as a pre-equalization algorithm for PS-QPSK. Because this algorithm inherently minimizes the cross correlation between the two orthogonal polarizations, the singularity problem is much less likely to occur as compared to the algorithm reported in [10]. In Fig. 3(a) and 3(b) we show the recovered constellation diagrams for 40.5Gb/s PM-QPSK and 40.5Gb/s PS-QPSK, respectively, for back-to-back measurements without additional loading noise.

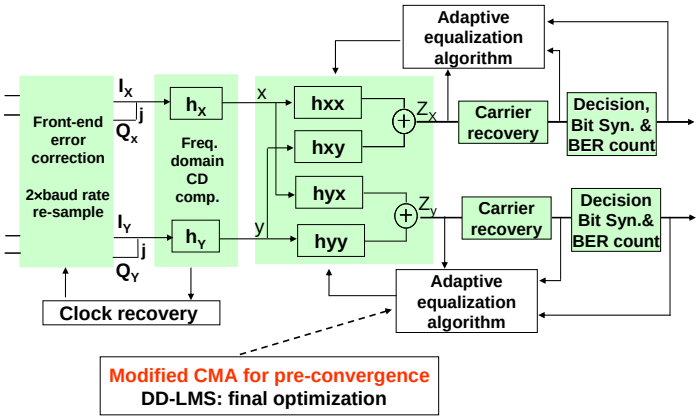

Fig. 2. Offline digital signal processing flow chart.

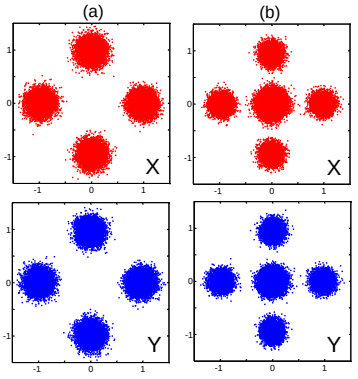

Fig. 3. Recovered constellation diagrams for back-to-back measurement of (a) 40.5Gb/s PM-QPSK and (b) 40.5Gb/s PS-QPSK.

Carrier frequency and phase recovery are implemented after the initial equalization stage. The frequency offset between the LO and the signal is estimated by using a constellation-assisted two-stage blind frequency search method [15]: the frequency offset is first scanned at a step size of 10MHz and then at a step size of 1MHz, and the optimal frequency offset is the

#146424 - $15.00 USD Received 22 Apr 2011; revised 12 May 2011; accepted 12 May 2011; published 18 May 2011

one that gives the minimum mean-square error. For each trial frequency, the carrier phase is first recovered (with best effort) by using a newly proposed two-stage phase estimation algorithm [16], and decisions made following this phase estimation are then used as reference signals for mean-square error calculation. Note that this frequency recovery method is applicable for any modulation format and can reliably recover carrier frequency by using only tens of symbols (64 were used in this experiment). The carrier phase is estimated by using a two-stage method: the carrier phase recovered from the previous symbol is used as an initial test phase angle. The "decided" signal made following this initial test phase angle is then used as a reference signal for a more accurate maximum-likelihood (ML) based phase recovery through a feed-forward configuration [16]. To reduce the probability of cycle slipping (no differential coding/encoding were applied in this experiment), sliding-window based symbol-by-symbol phase estimation is employed, and the window size is optimized for each case. Because for PS-QPSK only half of the symbols can be used for phase estimation for each polarization, whereas for PM-QPSK all the symbols are used for the phase estimation, for fair comparison, joint X- and Y-polarization phase estimation is only applied to PS-QPSK. For symbol-to-bit mapping, the principle described in [3] is used for PS-QPSK. For bit-error-ratio (BER) calculation, errors were counted over more than 1.2×10^6 bits of information.

2.2 Back-to-back results

Figure 4 shows a comparison of the back-to-back sensitivities in terms of E_b/N_0. At 10^{-3} BER, PS-QPSK shows 0.9dB improved sensitivity compared to PM-QPSK, assuming hard-decision FEC, agreeing well with the 0.97dB difference according to theory [4] and a recent demonstration of PS-QPSK subcarrier modulation [9]. The sensitivity difference increases to ~1.5dB at 10^{-5} BER, indicating that it is approaching the asymptotic sensitivity difference of 1.76dB first reported by Karlsson [3].

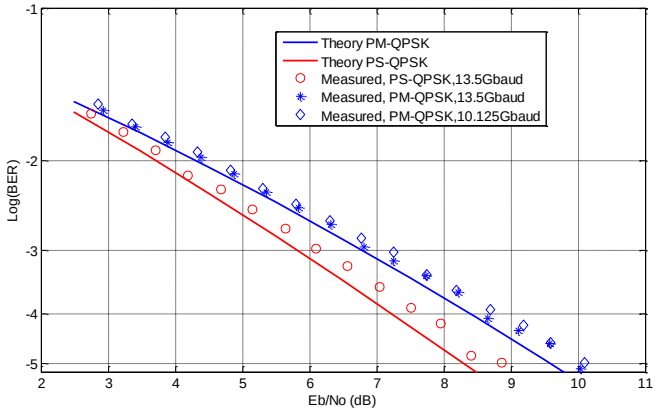

Fig. 4. Back-to-back sensitivity measurements for PS-QPSK and PM-QPSK.

We attribute the low implementation penalty for both modulation formats to several aspects of our experiment. The implementation penalty from the hardware (the electrical amplifier, the optical modulator, the receiver and the D/A resolution) was very small because the symbol rate was low compared to the available hardware bandwidth. The implementation penalty from the DSP was small (and smaller than that reported in [9] and [11]), because the constrained MMA and classic CMA were used only for pre-convergence for PS-QPSK and PM-QPSK, respectively, whereas the better-performing decision-directed LMS algorithm was used for the final equalization, resulting in ~0.5dB improvement of the sensitivity. In addition, improved two-stage feed-forward phase recovery algorithms were used in these experiments, resulting in negligible penalty at 10^{-3} BER for PM-QPSK and PS-QPSK with a laser linewidth <100kHz compared to the case of no laser phase noise.

#146424 - $15.00 USD Received 22 Apr 2011; revised 12 May 2011; accepted 12 May 2011; published 18 May 2011

3. Transmission experiment

A full transmission system set-up, as shown in Fig. 5, was used to investigate the nonlinear tolerance of PS-QPSK compared to that of PM-QPSK. The transmitters for the channel-under-test at 1550.14nm were the same as those used for the back-to-back sensitivity measurements for PS-QPSK and PM-QPSK. As shown in Fig. 5, an additional 19 C-band loading channels were combined with the signal channel in a 50GHz wavelength selective switch (WSS), such that there were five 50GHz-spaced channels on both sides of the channel-under-test as well as nine additional channels at 100GHz spacing to load the EDFAs (see spectrum inset in Fig. 5). The sets of odd and even loading channels were separately modulated with the same modulation format and bit-rate as the channel-under-test and were transmitted through 30km spools of standard single-mode fiber (SSMF) for decorrelation. The transmission line consisted of ten 100km spans of SSMF (average 20.5dB loss) and two-stage erbium-doped fiber amplifiers (EDFA), originally designed for a mid-stage attenuation of 5 to 10 dB to accommodate optical dispersion compensation. In the experiments, no optical dispersion compensation was used, so variable optical attenuators were inserted at the EDFA mid-stages after spans 1, 2, 4, 5, 7, 8, and 9 and adjusted to minimize gain tilt. The gain ripple from an individual EDFA was better than ± 0.7dB across the 20 channel spectrum. A wavelength blocker and WSS at the mid-stages of the EDFAs after spans 3 and 6, respectively, allowed for individual channel power equalization to compensate the accumulated EDFA gain ripple. The launch power into the spans could be varied from 10 to 19dBm (–3 to + 6dBm/ch), with a flat optical spectrum. After the tenth SSMF span, the signals were noise-loaded and the channel-under-test was selected with a WSS and sent to the previously described polarization- and phase-diverse coherent receiver.

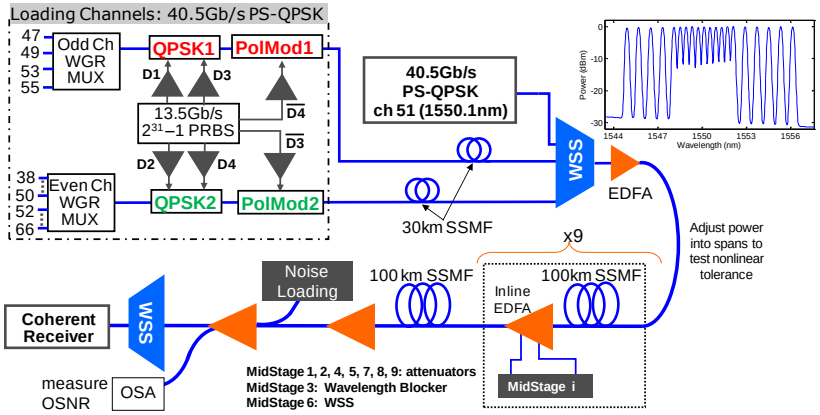

Fig. 5. Experimental set-up for PS-QPSK WDM transmission experiments over 10 × 100km SSMF. For PM-QPSK, polarization multiplexing stages replace the polarization modulators, and 10.125Gb/s data signals are applied to the QPSK modulators.

4. Transmission experiment results and discussion

For both modulation formats and a 9dB range of launch powers into the SSMF spans, we recorded the sampled and digitized data sets after the 1000km transmission for different levels of noise-loading of the channel-under-test. The received OSNRs, without additional noise loading after 1000km transmission, ranged from 16.3dB to 25.0dB for –3dBm/ch to + 6dBm/ch launch power, respectively. The DSP algorithms described in section 2.1 were then used to calculate curves of bit-error-ratio (BER) versus received OSNR, as shown in Fig. 6 for PS-QPSK. Similar curves for PM-QPSK also were obtained. In agreement with the WDM transmission simulations of [6,7] and experiment of [11], PS-QPSK clearly had higher

#146424 - $15.00 USD Received 22 Apr 2011; revised 12 May 2011; accepted 12 May 2011; published 18 May 2011

nonlinear tolerance. As shown in Fig. 6, at 4dBm/ch launch power, PS-QPSK had less than 2dB OSNR penalty relative to its back-to-back (at BER = 10^{-3}), whereas PM-QPSK had more than 4dB OSNR penalty relative to its back-to-back at the same 10^{-3} BER.

The curves of BER versus received OSNR for both modulation formats were then fitted to obtain the required OSNRs for 10^{-3} and $3.8\text{x}10^{-3}$ BER, and those results are plotted in Fig. 7. Note that, as indicated by the left-most x-axis tick label, the required OSNR for back-to-back in the WDM system setup is shown by the points furthest to the left. Allowing 1dB required OSNR penalty relative to each modulation format's own back-to-back sensitivity at 10^{-3} BER, PS-QPSK could tolerate approximately 1.6dB/ch higher launch power than PM-QPSK for the 10 × 100km transmission. Adding the 0.9dB improvement in back-to-back sensitivity for PS-QPSK to its higher nonlinear tolerance gives it a 2.5dB overall advantage in terms of OSNR margin compared to PM-QPSK. Of course, the sensitivity and nonlinear tolerance could be utilized to obtain significantly longer reach for PS-QPSK systems.

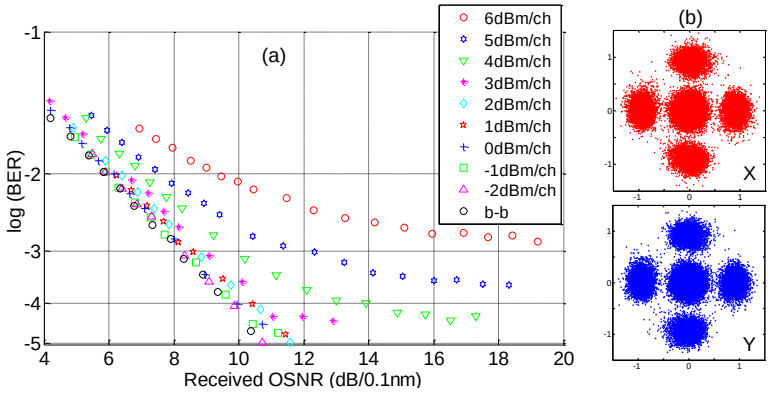

Fig. 6. (a) BER versus received OSNR for PS-QPSK after WDM transmission over 10 × 100km SSMF. (b) PS-QPSK constellation diagrams for 5dBm/ch and 18.3dB OSNR.

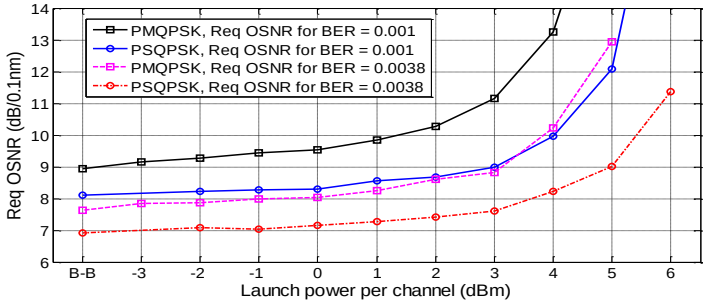

Fig. 7. Required OSNR for PS-QPSK and PM-QPSK (both at 40.5Gb/s) after WDM transmission over 10 × 100km SSMF for a range of launch powers into the spans.

5. Conclusion

We have experimentally demonstrated the PS-QPSK format in a typical terrestrial WDM system and compared its performance to polarization-multiplexed QPSK at the same bit rate of 40.5Gb/s. The low symbol rates of 13.5Gbaud for PS-QPSK and 10.125Gbaud for PM-QPSK were chosen to avoid bandwidth limitations of the transmitter and receiver components, and the PS-QPSK transmitter was implemented simply with a QPSK modulator followed by a polarization modulator. PS-QPSK and PM-QPSK were compared in a single-channel, back-to-back configuration, and for 10 × 100km WDM transmission over standard single-mode fiber with 50-GHz-spaced neighbor channels of the same modulation format. We also described a novel constrained multi-modulus algorithm for PS-QPSK, developed

#146424 - $15.00 USD Received 22 Apr 2011; revised 12 May 2011; accepted 12 May 2011; published 18 May 2011

concurrently to that of [11]. Our results demonstrate compelling advantages of PS-QPSK over PM-QPSK, including 0.9dB sensitivity improvement for back-to-back (at 10^{-3} BER) assuming conventional hard-decision forward-error-correction and up to 1.6dB higher launch power tolerance for a 1dB penalty in required OSNR relative to back-to-back. Thus, PS-QPSK may be considered a candidate for ultra-long haul transmission at 100Gb/s and beyond, where the transmission reach of higher-order modulation formats is currently a concern.

Acknowledgments

This work was supported, in part, by Science Foundation Ireland (SFI) under grant number 06/IN/I969.

#146424 - $15.00 USD Received 22 Apr 2011; revised 12 May 2011; accepted 12 May 2011; published 18 May 2011